Applying Fréchet distance to evaluate the discrepancy of product size distribution between single particle and monolayer multi-particle breakage

P Yu[a], W Xie[b], L X Liu[c,*], M S Powell[a]

[a] *Julius Kruttschnitt Mineral Research Centre, Sustainable Minerals Institute, University of Queensland, Indooroopilly, Brisbane, QLD 4068, Australia*

[b] *Camborne School of Mines, University of Exeter, Penryn Campus, Penryn, Cornwall, TR10 9FE, UK*

[c*] *Department of Chemical and Process Engineering, University of Surrey, Guildford, Surrey, GU27JP, UK*

Abstract

Single particle breakage characterisation at fine sizes for use in mill modelling has been addressed by only a few researchers and is not utilised in engineering design. This is mainly due to the challenge of accurately imparting a range of impact energies to sub-millimetre particles and then measuring the progeny size distribution for the tiny resultant mass. In order to fill this gap, a dispersed monolayer multi-particle breakage method was applied with a mini JK Drop weight tester in this work to extend the single particle breakage test from 16 mm down to 425 µm, covering a specific energy (Ecs) range of 0.1 - 2.5 kWh/t to provide a wide range of test conditions. A challenge that had to be addressed was switching from single particle to dispersed mono-layer due to the physical constraints of drop-height and drop mass in maintaining accuracy in input energy over the orders of magnitude required to apply the required specific range of energy input. As only a limited size range could be subjected to both single particle and mono-layer bed breakage, it was necessary to establish if the two testing techniques provide the same breakage results. A novel application of the Fréchet distance was successfully applied to quantitatively evaluate the discrepancy of progeny size distribution between single particle breakage and monolayer multiple particle breakage. Extrapolation of an empirical Fréchet distance model indicated that the application of dispersed mono-layer breakage below 2 mm provides an acceptable comparison with the single particle breakage applied to coarser sizes, thus facilitating the fitting of a single appearance function across this wide range of sizes and applied breakage energies.

Keywords: *Breakage characterisation, Fréchet distance, drop weight test, single particle breakage, multi-particle breakage*

*Corresponding author: Ph.: +44 (0) 1483686594, Email: l.x.liu@surrey.ac.uk

1. Introduction

Ore breakage characterisation is based on laboratory breakage testing work, with single particle breakage tests the most commonly used method. Single particle breakage is regarded as the primary breakage event in a grinding mill [1] and is also the key to mechanistic mill modelling that uses particle strength and strength distribution to model breakage [2]. Since the first single particle breakage test- the Bond Crushing Work Index (CWI) test was reported in 1947 [3], several single particle breakage tests were developed. These include the Twin Pendulum Test [4, 5], the Ultrafast Load Cell test (UFLC, also called Impact Load Cell) [6-8], the laboratory-scale compression crushing test [9, 10], the Short Impact Load Cell test (SILC) [11], the JK Drop Weight Test (JKDWT) [12], the SMC Test® [13], and the JK Rotary Breakage Test (JKRBT) [14]. Single particle impact breakage tests have been used to determine the appearance function, which is defined as the size distribution of the progeny after an impact event with a certain energy. This impact event may or may not have resulted in breakage of the particles involved. This is slightly different from the breakage function used in the population balance modelling, which defines the breakage function as the progeny size distribution of particles that undergo breakage.

The size range of particles (measured with K_{80}, the size at which 80% of particles by mass are smaller than that size) for single particle impact breakage tests is generally in the range of 10 mm to 60 mm (Fig. 1). For example, the size intervals used in the standard JKDWT are in the range of 13.2 mm – 63 mm [12]. The JKRBT can, however, test particles from 2.36 mm to 45 mm [14]. The size range from several millimetres to tens of millimetres matches a major portion of the feed ore size range for primary grinding mills such as AG/SAG mills. However, when dealing with finer grinding equipment such as ball mills, test results from large particle sizes cannot be used to predict the energy-appearance function relationship for mill feeds below 5 mm. This is because the appearance function, , is size-dependent, although sometimes it is assumed to be independent of particle sizes to simplify the characterisation work [16]. It has been demonstrated that considering the size dependence of the appearance functions will significantly improve the accuracy of prediction [2, 17, 18]. Therefore, single particle characterisation results obtained from larger particle sizes can't be used for modelling ball mills with a feed size below 2mm.

Extending the single particle breakage characterisation test to finer sizes will result in overwhelmingly intensive labour, as a minimum screening mass is required below which the sizing error is unacceptable. For example, if a Drop Weight Tester (DWT) is used for breakage characterisation of particles with a specific gravity 3.26 and size range -0.5+0.425 mm (average mass per particle = 1.67×10^{-4}g), up to 60,000 single particle breakage tests ($10/(1.67 \times 10^{-4})$) should be conducted for one test condition in order to obtain a mere 10g of product for screening. Thus, it is not viable to conduct single particle DWT breakage tests for very fine particles. The original Schönert breakage device (a small rotary breakage device operated in a low vacuum), upon which the Rotary Breakage Tester (RBT) design is based, is suited to conducting fine single particle breakage tests. Vogel and Peukert [19] and Ballantyne et al. [20] conducted such tests for fine particles with sizes from 2 mm to 125 μm. However, it is exceedingly slow to conduct tests, is tricky

to operate correctly and has an upper specific energy limit of about 0.8 kWh/t, rendering this unique device unsuitable for general ore characterisation.

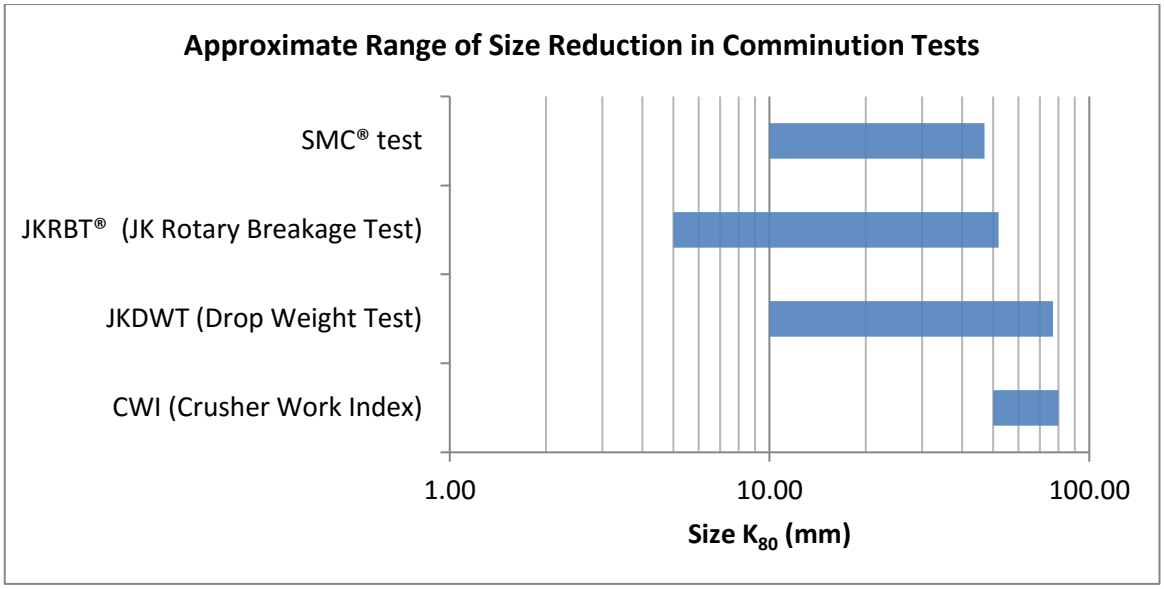

Fig. 1. Approximate range of size reduction in comminution tests

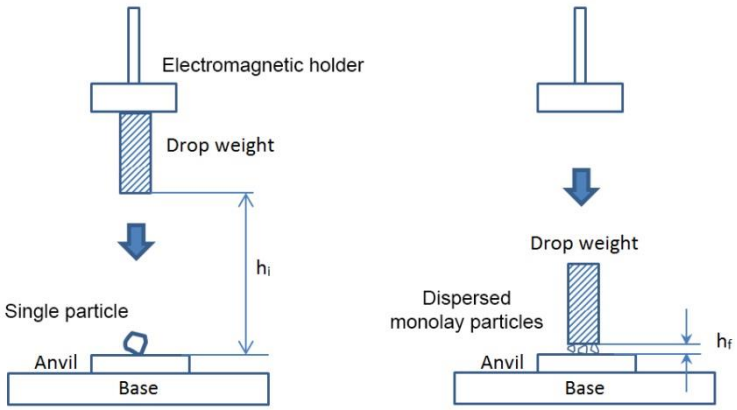

Fig. 2. Schematic diagram of Mini JK Drop Weight Tester and breakage energy calculation

Normally, continuous or locked-cycle grinding mill tests, such as ball mills, Vertimill®, IsaMill®, Lab-scale HPGR, AG/SAG pilot plant mills, are used for fine breakage characterisation [21]. Ballantyne et al. [22] compared the breakage products of fine particles (800 μm to 6 mm) with four devices: the single particle Schönert breakage device, the Fine Breakage Characterisation (FBC) test, the standard Bond Ball Work Index (BBWi) test, and the laboratory-scale HPGR test. Ballantyne et al. [22] used SSE_{75} (the energy required to generate one tonne of new -75 μm material) to develop quantitative energy-size relationships. Although continuous or locked-cycle grinding mill tests can extend the size down to millimetres, their results are inconsistent with single particle breakage conducted for coarser particles.

Barrios et al. [23] proposed a standard method using a small drop weight tester that drops a cylinder aligned on rails to strike a monolayer of particles to overcome the limitations of single particle testing at fine sizes. They proposed a stressing energy-size function which can describe fine particle breakage with parent sizes down to 100 μm. They did compare breakage for single and monolayers for two sizes (1.70-1.18 mm) at two energies (0.18 and 1.00 kwh/t), finding that the single particle gave a finer product size, the difference being greater at the low energy. However, they concluded that the difference was within the scatter of data used for fitting the breakage model, so no account was made of this difference in the modelling. The work covered only mono-layer particle breakage, but was presented together with drop-weight breakage data for larger sizes.

Reja et al. [24] investigated fine particle breakage (-11.2+1 mm) with monolayer particle breakage tests via the Short Impact Load Cell (SILC), using similar care in alignment to Barrios et al. [23] and extended the size specific energy (SSE) methodology to fine sizes (-4 mm). However, they did not analyse the errors between the monolayer particle bed breakage and the single particle breakage.

Aiming at a consistent and smooth extension from large single particle breakage to fine single particle breakage, we use dispersed monolayer multi-particle bed breakage tests to study the fine particle breakage (-8+0.425 mm) with the Mini JK Drop Weight Tester (Mini JKDWT). To evaluate the error of monolayer multi-particle bed breakage compared to single particle breakage, Fréchet distance is introduced to quantify the discrepancy of product size distribution between single particle breakage and monolayer multi-particle breakage. An error prediction model is developed based on the Fréchet distance theory. An alternative fine breakage characterisation technique which is equivalent to fine single particle breakage is proposed. The successful consistent extension to fine single particle breakage allows the development of a wide-range appearance function, which is more desirable in comminution modelling.

2. Experiment

To extend the rock size down to sub-millimetre in fine breakage characterisation, the Mini JK drop weight tester (Mini JKDWT) was used for ore breakage testing in this work. The Mini JK JKWT is a vertical drop

weight impact system with an electromagnet to hold the drop weight (Fig. 2), promoting good alignment of the impacting faces. The anvil for holding the particles has a diameter of 10 cm. The drop weights are flat-ended steel bars with different dimensions/masses so as to achieve the pre-determined specific energy levels. Table 1 lists the details of the masses and dimensions of the drop weight bars used. Comparing to the standard DWT, the maximum drop height and the maximum energy with the Mini JKRBT are much smaller and are around 61 cm and $4.785*10^{-6}$ kWh respectively.

Table 1. Drop weight bars of Mini DWT

Bars	Mass of Bar (g):	length (mm)	Diameter (mm)
No.1	99.64	15.80	32.00
No.2	170.52	45.30	24.90
No.3	426.93	69.10	31.90
No.4	1617.59	105.80	50.10
No.5	1901.98	124.00	49.90
No.6	2884.21	129.50	60.00

The required input energy for breakage is controlled through the gravitational potential energy of the drop weight.

The input energy for breakage [12] is:

$$E_{is} = \frac{0.0272 M_d (h_i - h_f)}{\overline{m}} \quad (1)$$

where, E_{is} is the input specific breakage energy (kWh/ton); M_d mass of drop weight (kg); h_i is the initial height (cm); h_f is the final height (cm); $\overline{m}$ is the average particle mass (g).

With a given drop weight and the required energy level, the height of the drop weight can be predetermined. For single particles with size class -16mm +13.2 mm, the maximum input specific energy is around 1 kWh/t. With fine particles, a monolayer multi-particle bed is used with the Mini JKDWT. A dispersed monolayer of particles was spread on the centre of the anvil surface to allow most of particles to be broken in a single impact. Great care was taken to minimise particle-particle contact and also to ensure that the drop weight face is parallel to the anvil so as to provide an even contact with all the particles.

The ore samples, a gold-copper porphyry deposits from Newcrest Cadia Hill, were sized into eight size fractions: -16+13.2 mm, -11.2+9.5 mm, -8+6.7 mm, -5.6+4.75 mm, -4+3.35 mm, -2+1.7 mm, -1+0.85 mm, -0.5+0.425 mm. The test were conducted at the following specific energy levels (kWh/t): 0.1, 0.5, 1.0, 1.5, 2.0, and 2.5. For each size fraction, particles were broken under impact at each of the six energy levels, giving 45 size-energy combinations. For each size-energy combination, a series of breakage tests were conducted to provide sufficient progeny mass for accurate determination of the product size. For size fractions greater than 8 mm, single particle breakage was used for each test and 30-50 repeat tests conducted

for each size-energy combination. For size fractions less than 3.35 mm, mono-layer bed breakage was used with 30 repeat tests conducted for each size-energy combination to cover the natural ore variation and experimental error.

It was necessary to establish if the two testing techniques, single particle and mono-layer bed, provide the same breakage results. Due to the physical constraints of drop-height and drop mass, only a limited size range could be subjected to both single particle and mono-layer bed breakage for direct comparison of the techniques. Thus, both single particle and mono-layer tests were conducted for only three of the size fractions: -4+3.35mm, -5.6+4.75 mm, and -8+6.7 mm. The number of particles in the multi-particle experiments was chosen such that the area that particles occupied on the Anvil is just smaller than the contact area of the smallest drop weight. This is to ensure that the drop weight can have full impact on the particles. The detailed test plan is shown in Table 2. In total, 3010 tests of 45 size-energy combinations were conducted.

Table 2. Number of particles per test and number of tests at different conditions

Ecs (kWh/t) / **Size, mm**	**0.1**	**0.5**	**1.0**	**1.5**	**2.0**	**2.5**
-16 +13.2 (single)	1×30*	1×30	1×30	-	-	-
-11.2 +9.5 (single)	1×30	1×30	1×30	1×30	1×30	1×30
-8 +6.7 (single)	1×30	1×30	1×30	1×30	1×30	1×30
-8 +6.7 (multiple)	3×50	3×50	3×50	3×50	3×50	3×50
-5.6 +4.75 (single)	1×50	1×50	1×50	1×50	1×50	1×50
-5.6 +4.75 (multiple)	5×50	5×50	5×50	5×50	5×50	5×50
-4 +3.35 (single)	1×120	1×120	1×120	1×120	1×120	1×120
-4 +3.35 (multiple)	5×50	5×50	5×50	5×50	5×50	5×50
-2 +1.7 (multiple)	50×30	50×30	50×30	50×30	50×30	50×30
-1 +0.85 (multiple)	100×80	300×30	300×30	300×30	300×30	100×80
-0.5 +0.425 (multiple)	2000×30	2000×30	2000×30	2000×30	2000×30	2000×30

* Number of particles per test × number of repeated tests at different conditions

For -2 mm particles, the monolayer multi-particle bed breakage method was applied. In each test, all the particles are put on the anvil forming a dispersed monolayer of particles with no overlap. For size classes -1+0.85 mm and -0.5+0.425 mm, the number of particles per test is estimated based on the total mass of the testing sample. For other size classes, the number of particles per test was counted.

The procedures for breakage test using the Mini JKDWT are as follows. Firstly, Screen the test samples into the different size fractions listed in Table 2; (2) Select a size-energy combination from Table 2; (3) For each size class, choose a drop weight and calculate the predetermined height; (4) Conduct a series of drop weight tests for the given size-energy combination. For example, for multiple particle breakage under the condition where the input size fraction is -5.6+4.75 mm and Ecs is 0.1 kWh/t, 50 repeat tests are conducted.

In each test, 5 particles form a dispersed monolayer and are broken in one impact. The breakage products of all the 50 tests are collected; (5) Collect all the products under the given size-energy combination and size them to get product size distribution; (6) Select another size-energy combination and go to step (3) until all size-energy combinations are completed.

3. Results and discussion

3.1 Effect of specific energy and original feed size on breakage

Some of the typical breakage product size distribution (one feed size -500+425μm to represent the fine end and another feed size -11.2+9.5mm to represent the coarse end) are shown in Fig. 3 and Fig. 4. It is apparent that with the increase of specific energy and the decrease of original rock sizes, the products become progressively finer. The product size distributions of different feed sizes at Ecs 1.0 kWh/t are compared in Fig. 5. It is noted in Fig. 5 that, at the same specific energy of 1 kWh/t, the shape of the particle size distribution changes dramatically as the original size decreases. It is also quite clear from the data for feed particles with size below 4 mm that such steepening is partially the result of a significant fraction of the particles not breaking under specific energy of 1 kWh/t. This illustrates that the appearance function derived from these tests is dependent on the feed size, which has been reported for other ores [25].

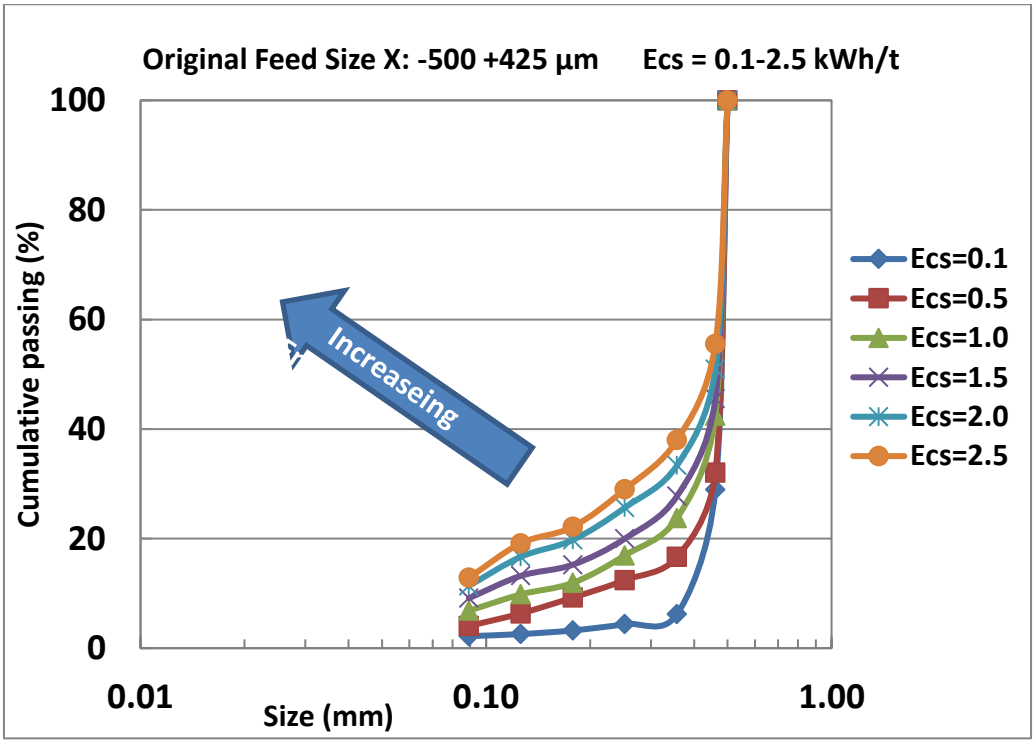

Fig. 3. Product size distribution of X= -500+425 μm at different Ecs

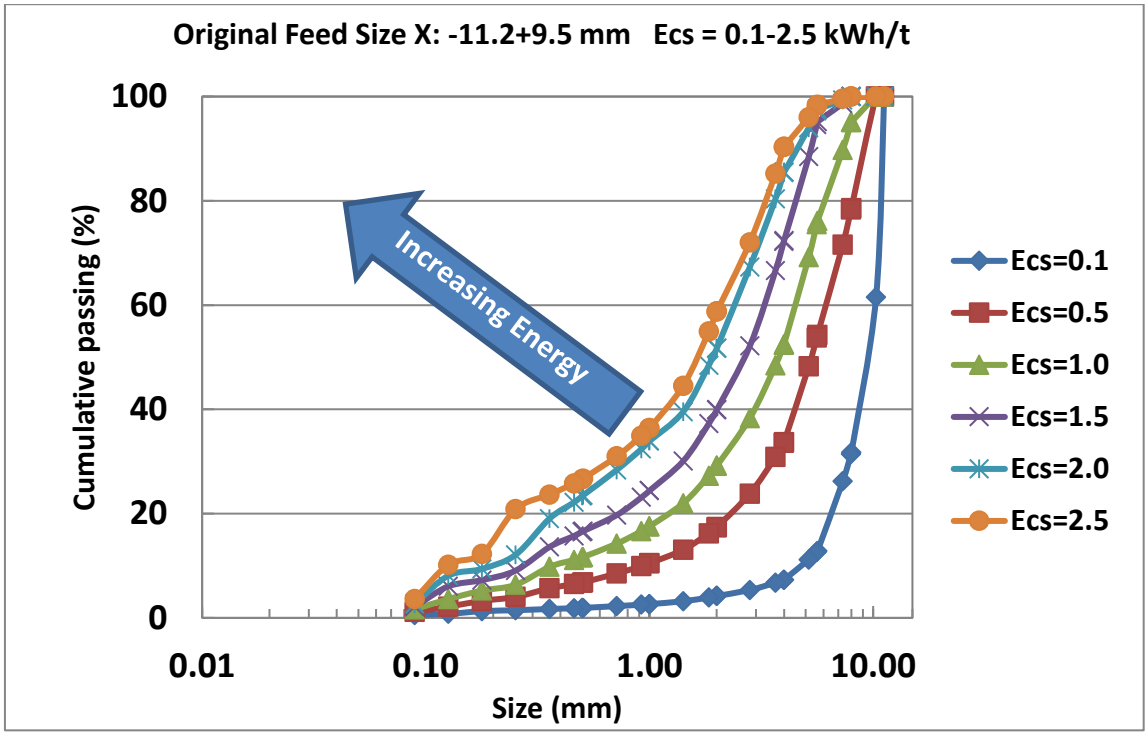

Fig. 4. Product size distribution of X= -11.2+9.5 mm at different Ecs

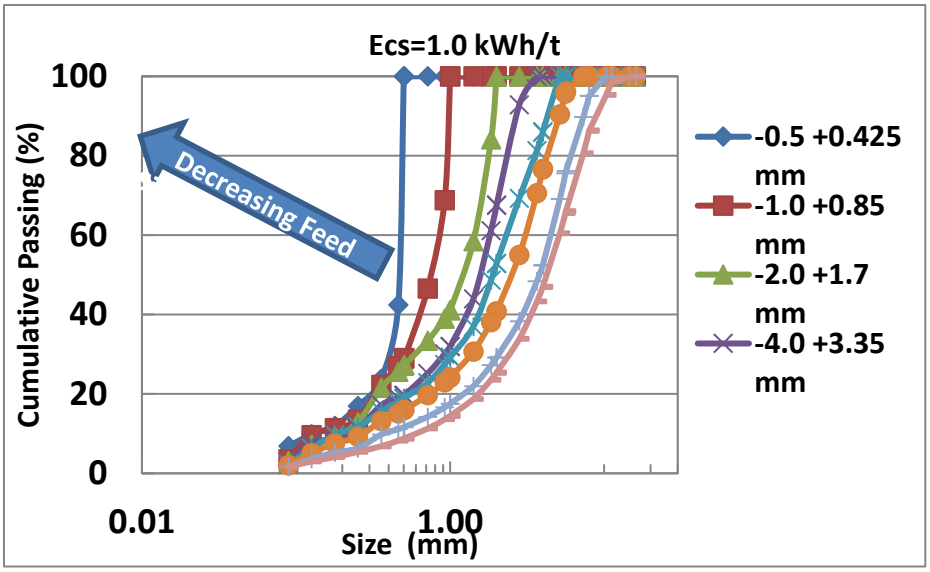

Fig. 5. Product size distribution of Ecs=1.0 kWh/t at different original feed size X

3.2 Single particle breakage versus monolayer multiple particle breakage

To show whether there is a difference between single particle breakage and multiple particle breakage, size fractions -8 +6.7 mm, -5.6 +4.75 mm and -4+3.35 mm were tested with the two breakage methods. Some of the results for size fraction -4+3.35 mm are presented in Fig. 6, showing that multiple particle breakage resulted in slightly coarser products, but the difference is rather small in this case. The full analysis of all the results is presented in Section 3.3.

Ideally with monolayer multiple particle breakage testing, the energy of the drop weight should be evenly distributed to each particle. However, there are particle shape differences among particles which can lead to uneven contact between the drop weight with each of the particles in the particle layer. Consequently, the applied energy will not be distributed evenly among all the particles. At very low impact energy, it is expected that some smaller particles may not be impacted by the drop weight as larger particles would support the drop weight. This was also presented in the work of Barrios et al. [23].

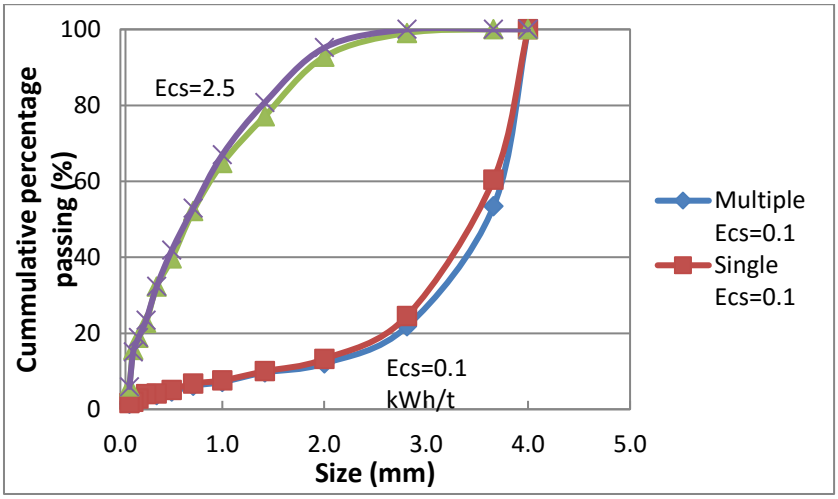

Fig. 6. Comparison between the single particle breakage and the monolayer multi-particle bed breakage for size fraction -4+3.35 mm

3.3 Applying Fréchet distance

To compare the two size distributions quantitatively, the Fréchet distance, a quantitative measure of the difference, was introduced [26]. The Fréchet distance is a measure of the likeness between curves with the location and order of the points along the curves considered. Supposing α and β are two polylines and a man, who is walking along α, is taking his dog for a walk on an extendable leash, but the dog follows its own nearby path along β. They are moving continuously from one end of the polylines to the other end with the man minimising the length of the leash at all times. Their motion is monotonic (i.e. the not moving backward is a constraint imposed on the motion). The Fréchet distance between α and β is the minimum leash length needed, it is presented as follows [27]:

$$\mathcal{F}(\alpha,\beta) = \min_{f:[0,1]\to\alpha, g:[0,1]\to\beta} \max_{t} \; d\left(f(t), g(t)\right) \tag{2}$$

where *f* and *g* are continuous non-decreasing functions which define the positions of the man and the dog on the curves at every moment.

Wylie and Zhu [28] presented the discrete Fréchet distance to compute the Fréchet distance between two polygonal curves:

$$d_F(f,g) = \min_{\alpha:[1:m+n]\to[0:m],\beta:[1,m+n]\to[0:n]} \max_{s\in[1:m+n]} d\left(f(\alpha(s)), g(\beta(s))\right) \tag{3}$$

where, d_F is the discrete Fréchet distance; *d(a, b)* represents the Euclidean distance between two points *a* and *b*; *f* is a polygonal curve: $f : [0 : m] \to R^k$; *g* is a polygonal curve: $g : [0 : n] \to R^k$; m and n are the numbers of nodes in curve *f* and curve *g*; *s* is the parameter in [1: m+n]; α and β range over all discrete non-decreasing onto mappings of the form $\alpha : [1 : m + n] \to [0 : m]$, $\beta : [1 : m + n] \to [0 : n]$. Curve *f* and *g* must be re-parameterized from the number of monotonic combinations (m +n) to the number of nodes in its curve (m or n) because the discrete Fréchet distance looks at all discrete monotonic parameterizations over the nodes of the two polygonal curves. The minimum of all re-parameterizations is the discrete Fréchet

distance (Eq.(3)). The Fréchet distance is more applicable in the continuous curve similarity analysis than other statistical methods such as the Weighted Least Square (WLS) method and the Root Mean Square Distance (RMSD) method [29]. The WLS method disregards the orientation of the curve and is suitable for a discrete set of data points. In addition, The WLS needs to know the exact weight which is difficult to estimate precisely [30]. Compared with the WLS, the Fréchet distance highlights the maximum deviation of the two lines and thus is more meaningful and expressive.The RMSD method is normally applied to analyse the similarity of three-dimensional structures and is not suitable for curve similarity analysis [31].

The minimum size tested in single particle mode was -4+3.35 mm due to a large number of tests and extremely low drop heights required for the next finer size class. All the breakage data of the single particle breakage and the monolayer multi-particle breakage at different energy levels for feed sizes -4+3.35 mm, -5.6+4.75 mm and -8+6.7 mm are plotted in Fig. 7. Eq. (3) and the corresponding MATLAB codes were used to calculate the Fréchet distances between the product size distribution (PSD) curves of single particle breakage and the corresponding monolayer multi-particle breakage. Because the values of compared curves are the accumulative percentages passing (%), as a measure of the difference between two curves, the Fréchet distance, in this case, can be considered as the error of the accumulative percentage passing (%). All the Fréchet distance values (%) are marked on the figures (Figs. 7(a)-7(c)).

It is seen from Fig. 7 that the monolayer multi-particle breakage results in coarser products than the single particle breakage. Fig. 8 shows that with increasing specific energy Ecs and decreasing particle size, the Fréchet distance decreases. In other words, the difference between the single particle breakage and monolayer bed breakage decreases with decreasing particle size, indicating that the monolayer bed breakage should only be utilised to substitute single particle breakage for fine particles below a few millimetres in size. The above phenomenon can be explained by the following mechanism. With large particles, other than the shape difference between the particles in the same size fraction, the absolute size difference between the particles is also larger than that for small particle size fractions. Thus, the difference between multi-particle bed breakage and single particle breakage for larger size fractions is higher (a larger Fréchet distance), as shown in Fig. 8. With increasing input energy Ecs, the discrepancy caused by the particle shape and size difference is reduced (Fréchet distance decreases as Ecs increases, as shown in Fig. 8), as the drop weight can crush all the particles at the high input specific energy. In contrast, if the input energy is too small to break all the particles, the breakage product of multi-particles will be coarser due to the survival of some protected particles.

Based on the experimental data, a prediction model as shown in Eq. (4) for the Fréchet distance between the dispersed monolayer multi-particle breakage and the single particle breakage was developed:

$$Fréchet = ae^{\left[-\frac{1}{2}\left(\frac{ln(X)-b}{c}\right)^2+\left(\frac{ln(Ecs)-d}{e}\right)^2\right]} \quad (4)$$

where, a,b,c,d and e are parameters and Ecs is the specific energy (kWh/t) and X (mm) is the feed size for the breakage test. With the cut-and-trial fitting method and the aid of the MATLAB fitting toolbox the

model is illustrated in Fig. 9, showing that the Fréchet distance decreases with increasing specific energy Ecs and decreasing feed size.

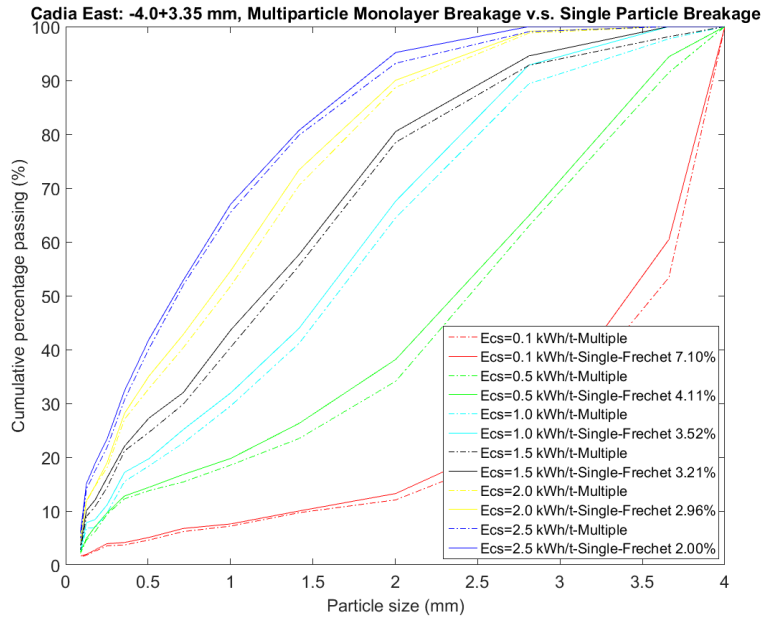

(a)

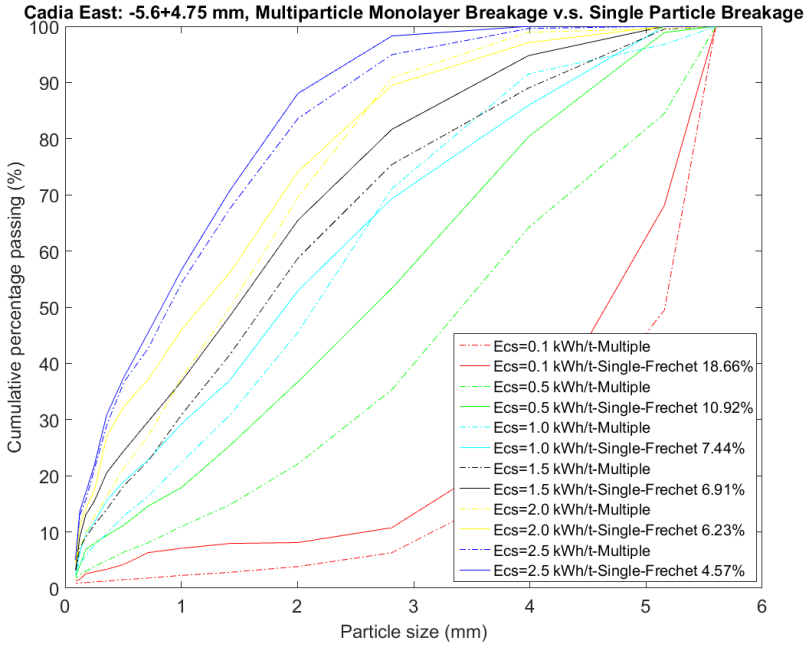

(b)

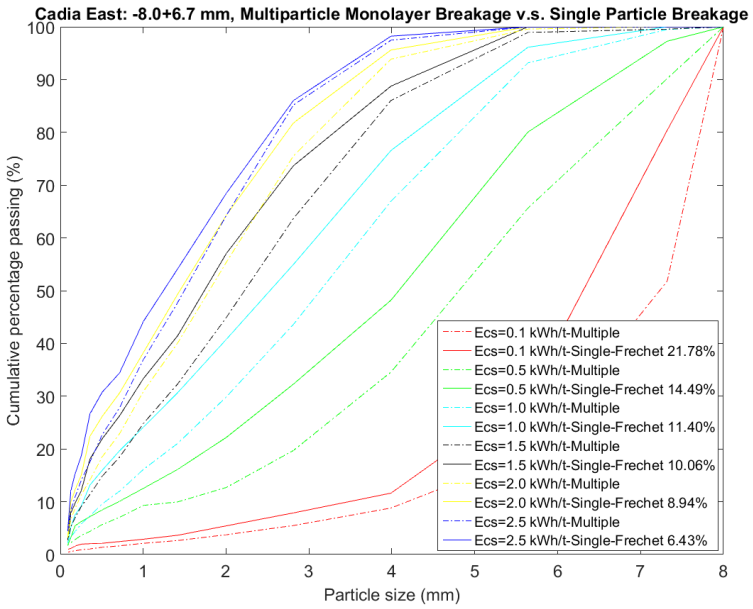

(c)

Fig. 7. Comparison of product size distribution of monolayer multi-particle breakage and single particle breakage using the Fréchet distance. (a) Size -4+3.35 mm; (b) Size: -5.6+4.75 mm; (c) Size: -8+6.7 mm

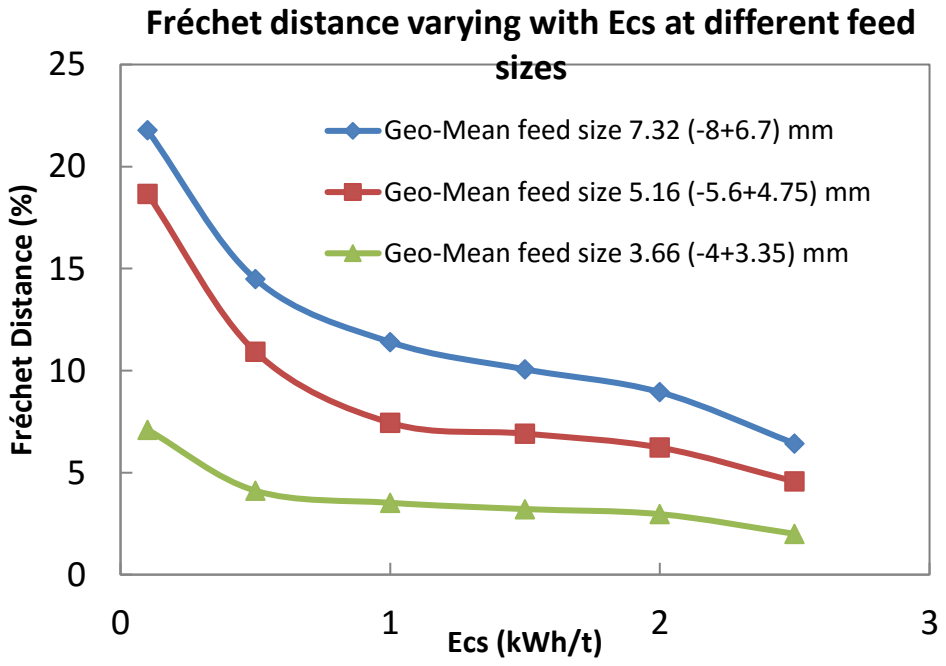

Fig. 8. Fréchet distance curve comparison between different feed sizes

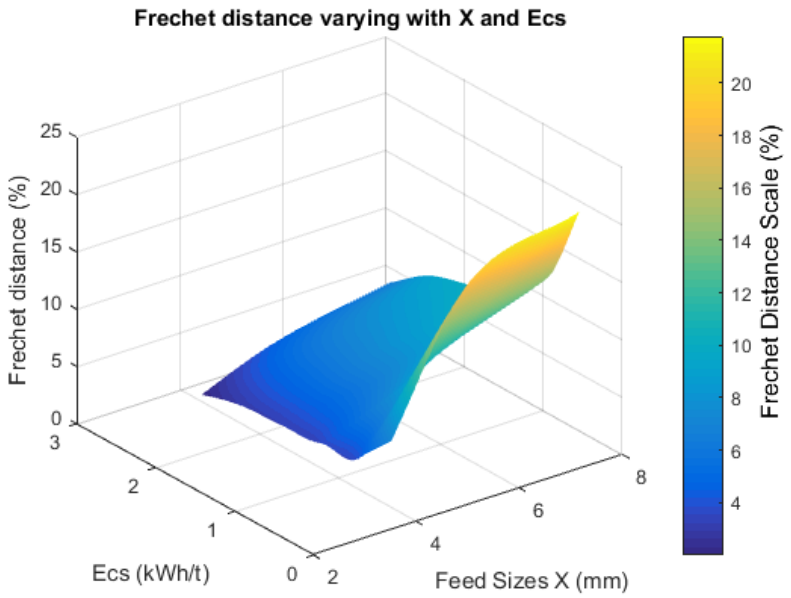

Fig. 9. Fréchet distance prediction model

The parameters obtained in this work are listed in Table 3. It is expected that for different ores the equation form of the model (Eq.(4)) should be the same but the parameter values (Table 3) may be different. Ongoing validation work could establish if there is a significant difference in the projected error model down to finer sizes with different ores. If a consistent relationship is found for this model form across different ores, then the proposed relationship would be of use in defining at what size the single particle breakage tests can switch to mono-layer breakage, dramatically reducing the number of tests required for each new ore.

Table 3. Parameters for Fréchet distance estimation (R^2=0.99)

a	b	c	d	e
27.95	1.94	-0.42	-4.36	3.20

Using this model the error is extrapolated to the finer sizes. It is estimated that the error (the Fréchet distance) for dispersed monolayer multi-particle breakage test for 2 mm is 0.3579 at Ecs = 0.01 kWh/t and 0.0918 at Ecs = 2.5 kWh/t respectively. That means the error in the cumulative percentage passing of the PSD of monolayer multi-particle breakage test at the combination of X = 2mm and Ecs = 0.01 kWh/t is 0.3579% and the error at the combination of X = 2 mm and Ecs = 2.5 kWh/t is 0.0918%. From the trends shown in Fig. 9, the error caused by a multi-particle breakage (measured as the Fréchet distance) is less than 0.3579% for particles below 2 mm. Therefore, the dispersed multi-particle monolayer breakage test can be used as the substitute for single particle breakage when X is smaller than 2mm.

4. Conclusions

To extend the monolayer single particle breakage test proposed by Barrios et al. [23] down to sub-millimetres size range, the dispersed monolayer multi-particle bed breakage method was applied by using

the Mini JK drop weight tester. Fréchet distance, an error evaluation index, was successfully applied to estimate the difference between single particle breakage and monolayer multiple particle breakage. The greatest advantage of using the Fréchet distance is that it can discriminate between different size distributions. A Fréchet distance model was also developed based on the experimental data from one type of ore. The model predicted that for fine particles with sizes below 2 mm, the dispersed monolayer multiple particle breakage method can substitute single particle breakage test with acceptable errors. If the Fréchet distance model is applied, the work performed using multi-particle monolayer can be translated to single particle breakage for a wider range of sizes.

The Fréchet distance model proposed in this paper is based on one ore. The work was conducted as only part of a wider PhD on mill modelling and took months to complete over 3000 painstaking experiments, so it was not feasible to conduct for more ores at this stage. Future work should look at a range of ores to validate if the monolayer multi-particle breakage test for -2mm can be used to replace the single particle test using the experimental technique and mathematical methodology presented in this paper, and to confirm if the parameters are ore specific. If it is validated for a wide range of ores, then a simpler and viable fine breakage characterisation technique will be available for fine grinding modelling.

Acknowledgements

The authors wish to acknowledge the financial support of the Commonwealth Scholarship from the Australian Government and Scholarships from The University of Queensland. The authors wish to acknowledge the partial financial support on supervision from AMIRA P9P project. The review and advice on this paper by Dr Marko Hilden are highly appreciated.

References

[1] R.P. King, Modeling and simulation of mineral processing systems, Butterworth-Heinemann Linacre House, Jordan Hill, Oxford OX2 8DP United Kingdom, 2001.

[2] R.M. Carvalho, L.M. Tavares, Leaping forward in SAG and AG mill simulation using a mechanistic model framework, in: K. Major, B.C. Flintoff, B. Klein, K. McLeod (Eds.) SAG 2011: International Autogenous Grinding, Semiautogenous Grinding and High Pressure Grinding Rolls TechnologyVancouver, B.C. Canada, 2011, pp. 1-26.

[3] F.C. Bond, Crushing tests by pressure and impact, Trans AIME, Am. Inst. Min. Metall. Petrol. Eng. , 169 (1947) 58-66.

[4] S.S. Narayanan, Development of a laboratory single particle breakage technique and its application to ball mill modelling and scale-up, JKMRC, School of Engineering, the University of Queensland, Brisbane, QLD, Australia, 1985, pp. 466.

[5] S.S. Narayanan, W.J. Whiten, Determination of comminution characteristics from single particle breakage tests and its application to ball mill scale-up, Trans. Inst. Miner. Metall., 97 (1988) C115-C124.

[6] R.P. King, F. Bourgeois, Measurement of fracture energy during single-particle fracture, Minerals Engineering, 6 (1993) 353-367.

[7] L.M. Tavares, R.P. King, Measurement of the load-deformation response from impact breakage of particles, International Journal of Mineral Processing, 74, Supplement (2004) S267-S277.

[8] R. Weichert, J. Herbst, An ultrafast load cell for measuring particle breakage, World Congress Particle Technology: Part II. Comminution, 1986, pp. 3-15.

[9] C.M. Evertsson, Size reduction in cone crushers, Minerals Engineering Conference'99 Falmouth, England, 1999.

[10] C.M. Evertsson, Cone Crusher Performance, Department of Machine and Vehicle Design, The Chalmers University of Technology, Göteborg, Sweden, 2000.

[11] F.S. Bourgeois, G.A. Banini, A portable load cell for in-situ ore impact breakage testing, International Journal of Mineral Processing, 65 (2002) 31-54.

[12] T.J. Napier-Munn, S. Morrell, R.D. Morrison, T. Kojovic, Mineral comminution circuits: their operation and optimisation, Julius Kruttschnitt Mineral Research Centre, the University of Queensland, Indooroopilly, Brisbane, Australia, 1996.

[13] S. Morrell, Predicting the specific energy of autogenous and semi-autogenous mills from small diameter drill core samples, Minerals Engineering, 17 (2004) 447-451.

[14] F. Shi, T. Kojovic, S. Larbi-Bram, E. Manlapig, Development of a rapid particle breakage characterisation device – The JKRBT, Minerals Engineering, 22 (2009) 602-612.

[15] L.X. Liu, S. Palaniandy, M. Powell, A review of technical gaps and challenges in modelling fine grinding Comminution '14: 9th International Comminution SymposiumCape Town, South Africa, 2014.

[16] Ö. GENÇ, L. ERGÜN, H. BENZER, Single particle impact breakage characterization of materials by drop weight testing, Physicochemical Problems of Mineral Processing, 38 (2004) 241-255.

[17] F. Shi, T. Kojovic, Validation of a model for impact breakage incorporating particle size effect, International Journal of Mineral Processing, 82 (2007) 156-163.

[18] P. Yu, W. Xie, L.X. Liu, M.S. Powell, The development of the wide-range 4D appearance function for breakage characterisation in grinding mills, Minerals Engineering, 110 (2017) 1-11.

[19] L. Vogel, W. Peukert, Breakage behaviour of different materials - construction of a mastercurve for the breakage probability, Powder Technology, 129 (2003) 101-110.

[20] G.R. Ballantyne, W. Peukert, M.S. Powell, Size specific energy (SSE)—Energy required to generate minus 75 micron material, International Journal of Mineral Processing, 136 (2015) 2-6.

[21] F.O. Verret, G. Chiasson, A. Mcken, SAG mill testing - an overview of the test procedures available to characterize ore grindability, The 5th International Conference on Autogenous and Semiautogenous Grinding Technology, SAG 2011Vancouver, Canada, 2011.

[22] G.R. Ballantyne, F. Shi, B. Bonfils, M.S. Powell, Comparison of single particle, Bond and bed tests for fine particle ore breakage characterisation, Comminution '14: 9th International Comminution Symposium, Cape Town, South Africa, 2014.

[23] G.K.P. Barrios, R.M. de Carvalho, L.M. Tavares, Extending breakage characterisation to fine sizes by impact on particle beds, Mineral Processing and Extractive Metallurgy, 120 (2011) 37-44.

[24] Y. Reja, G.R. Ballantyne, B. Bonfils, M.S. Powell, Double impact breakage: Comparison and extension of size specific energy methodology, 14th European Symposium on Comminution and Classification (ESCC) Gothenburg, Sweden, 2015.

[25] L.M. Tavares, P.B. das Neves, Microstructure of quarry rocks and relationships to particle breakage and crushing, International Journal of Mineral Processing, 87 (2008) 28-41.

[26] M. Frécht, Sur quelques points du calcul fonctionnel, Rendiconti del Circolo Mathematico di Palermo, 22 (1906) 1-74.

[27] Efrat, Guibas, S. Har-Peled, Mitchell, Murali, New Similarity Measures between Polylines with Applications to Morphing and Polygon Sweeping, Discrete & Computational Geometry, 28 (2002) 535-569.

[28] T. Wylie, B. Zhu, Following a curve with the discrete Fréchet distance, Theoretical Computer Science, 556 (2014) 34-44.

[29] S.L. Seyler, A. Kumar, M.F. Thorpe, O. Beckstein, Path Similarity Analysis: A Method for Quantifying Macromolecular Pathways, PLOS Computational Biology, 11 (2015) e1004568.

[30] T.J. Cleophas, A.H. Zwinderman, Weighted Least Squares, Machine Learning in Medicine: Part Three, Springer Netherlands, Dordrecht, 2013, pp. 95-103.

[31] O. Carugo, S. Pongor, A normalized root-mean-square distance for comparing protein three-dimensional structures, Protein Science, 10 (2001) 1470-1473.